Hysteresis Loops of Magnetically Coupled Multilayers - Experiment and Calculations

M. Czapkiewicz[1]*, T. Stobiecki[1], R. Rak[1], J. Wrona[1] and C. G. Kim[2]

[1]Department of Electronics, University of Science and Technology, 30-059 Krakow, Poland
[2]Department of Materials Engineering, Chungnam National University, Daejon, Korea

In this paper calculations of magnetisation and magnetoresistance characteristics of the Spin Valve (SV) and Pseudo Spin Valve (PSV) spintronics structures are reported and compared with the experimental data. The magnetisation reversal process was analysed with respect to the Stoner-Wohlfahrt model of total surface energy in terms of uniaxial anisotropy, exchange coupling between ferromagnetic layers, unidirectional exchange anisotropy of pinned layer (modelled by exchange coupling between magnetisation of pinned layer and net magnetisation of antiferromagnetic layer with high anisotropy). The numerical simulation of the model to the experimental magnetisation data yielded the above parameters for SV and PSV structures. These parameters were used to more sophistically micromagnetic modelling tool originating from the project called Object Oriented Micromagnetic Framework. Influence of the shape anisotropy of the Magnetic Tunnelling Junction cell used in MRAM was simulated by means of micromagnetic simulations. Results were compared to those obtained from the spot Kerr measurements.

Key words : micromagnetics, spintronics, magnetometry, giant magnetoresistance

1. Introduction

Optimisation of Giant Magnetoresitance (GMR) and Tunnelling Magnetoresistance (TMR) effects in artificial superlattice systems are the subject of basic and practical research studies due to their applications in spintronics. The shape of the resistance hysteresis R(H) should be fitted to the real implementation such as high sensitive linear magnetic field sensor, nanoscale head for reading magnetic media or a non-volatile memory cell of MRAM array. Functionality of such magnetoresitivity elements depend directly on the shape of the magnetisation hysteresis loop, because magnetoresitivity effects are originated from the magnetic reversal process. Understanding of magnetic reversal process is a key for opening possibilities of optimisation of spintronics elements.

2. Spin Valve element - single domain model

Spin Valve [1] name originates from asymmetrical, shifted hysteresis loop of magnetisation and magnetoresistance. Such multilayer systems consist of a soft ferromagnetic "free" layer (FF), coupled magnetically to another ferro-

magnetic "pinned" layer (FP) across a non-ferromagnetic spacer (S). The FP layer exhibits unidirectional exchange anisotropy due to the pinning of magnetisation resulting from the exchange interaction between ferromagnetic layer FP and antiferromagnetic grains of exchange-biasing (AF) layer with induced anisotropy of magnetic subnets [2]. Additional top and bottom layers are prepared to protect and ensure quality growth during deposition.

Simple single domain model, assuming coherent rotation of magnetisation vector of each magnetic layer was used for estimation of basic magnetic properties of SV system. Total surface energy model can be given by the following formula:

$$E(\theta_1, \theta_2, \theta_{AF}) = -J \cos(\theta_2 - \theta_1) - J_{EB} \cos(\theta_1 - \theta_{AF})$$
$$-t_1\mu_0 M_{S1}(H_X \cos\theta_1 + H_Y \sin\theta_1) - t_2\mu_0 M_{S2}(H_X \cos\theta_2 \quad (1)$$
$$+ H_Y\sin\theta_2) - K_1 t_1\cos^2\theta_1 - K_2 t_2\cos^2\theta_2 - \hat{K}_{AF} t_{AF}\cos^2\theta_{AF},$$

where θ_1, θ_2 are the magnetisation angles as shown in Fig. 1. The first term gives the exchange coupling between both ferromagnetic layers, FF and FP, over the spacer interlayer, with exchange coupling parameter J. The second term corresponds to the exchange anisotropy energy J_{EB} between FP and AF layer. Next two terms represent the Zeeman energy of the magnetic layers. The last three
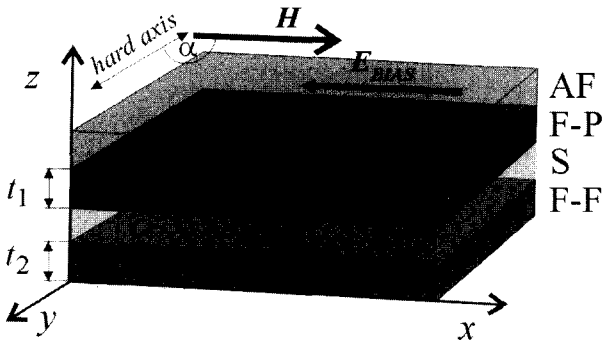
Fig. 1. Top type Spin Valve structure.

terms represent energy of uniaxial anisotropy of the ferromagnetic layers and antiferromagnetic layer, where K_1, K_2 and K_{AF} are the anisotropy constants and t_1, t_2 and t_{AF} are the thickness of FP, FF and AF layer respectively.

Numerical reconstruction of hysteresis loop was done by search of angles θ_1, θ_2 which fulfils a local minimum of the total energy function (1). This step was repeated for each external magnetic field values increasing in the given range. The same procedure was repeated for decreasing field. Average magnetisation of the sample was calculated from

$$M(H) = M(\theta_1, \theta_2) = (t_1 M_{S1} \cos\theta_1 + t_2 M_{S2}\cos\theta_2)/(t_1+t_2),$$
(2)

where M_{S1} and M_{S2} are the magnetisation saturation of ferromagnetic layers, hence GMR or TMR effect was obtained from the following formula:

$$R(H) = R(\theta_1,\theta_2) = R_{\uparrow\uparrow} + (\Delta R/2) [1-\cos(\theta_1-\theta_2)],$$
(3)

where $R_{\uparrow\uparrow}$ is a resistance of sample with parallel magnetisation vectors, ΔR is a difference between resistance $R_{\uparrow\uparrow}$ and $R_{\uparrow\uparrow}$ (resistance of sample with antiparallel magnetisation vectors).

Calculations for the top-type SV structure (AF layer at the top of the stack): Si/Al₂O₃/Ta/Co(4.4)/Cu(2.3)/Co(4.4)/FeMn(10)/Ta with field along easy axis ($H_Y = 0$) are shown in Fig. 2a (magnetisation reversal process) and Fig. 2b (GMR effect). Simulation is compared to magnetisation data measured by Resonance Vibrating Sample Magnetometer [3] and resistivity measured in current in plane geometry (CIP).

The following parameters were obtained: exchange constant $J = 7.9 \times 10^{-6}$ J/m², $J_{EB} = 94 \times 10^{-6}$ J/m² and uniaxial anisotropy $K_1 = 580$ J/m³, $K_{AF} = 80 \times 10^3$ J/m³. $K_{AF}{\cdot}t_{AF}$ value is higher than J_{EB}, thus FP layer is "pinned" in one direction. This effect occurs due to the external field of 1.25 kAm⁻¹ applied during RF-deposition to obtain unidirectional orientation of AF subnets coupled to previously deposited FP layer.

Another more complex example of bottom-type SV with multilayer structure with buffer Si/Ta(5)/Cu(10)/Ta(5)/Ni₈₀Fe₂₀(2)/Cu(5), AF layer Ir₂₅Mn₇₅(10), FP layer Co₇₀Fe₃₀(2.5), isolator spacer AlOₓ(1.5), FF layer Co₇₀Fe₃₀(2.5)/Ni₈₀Fe₂₀(10) and capping Ta(5) can be used as memory cell in M-RAM. Thin isolator barrier provides Tunnelling Magnetoresistance effect and low magnetic coupling between FF and FP layer.

Thermal treatment is necessary to obtain the SV effect, induced by magnetic ordering of AF layer located under FP layer. Sample was annealed in vacuum at 300 °C for 1 hour in the external magnetic field of 80 kA/m, followed
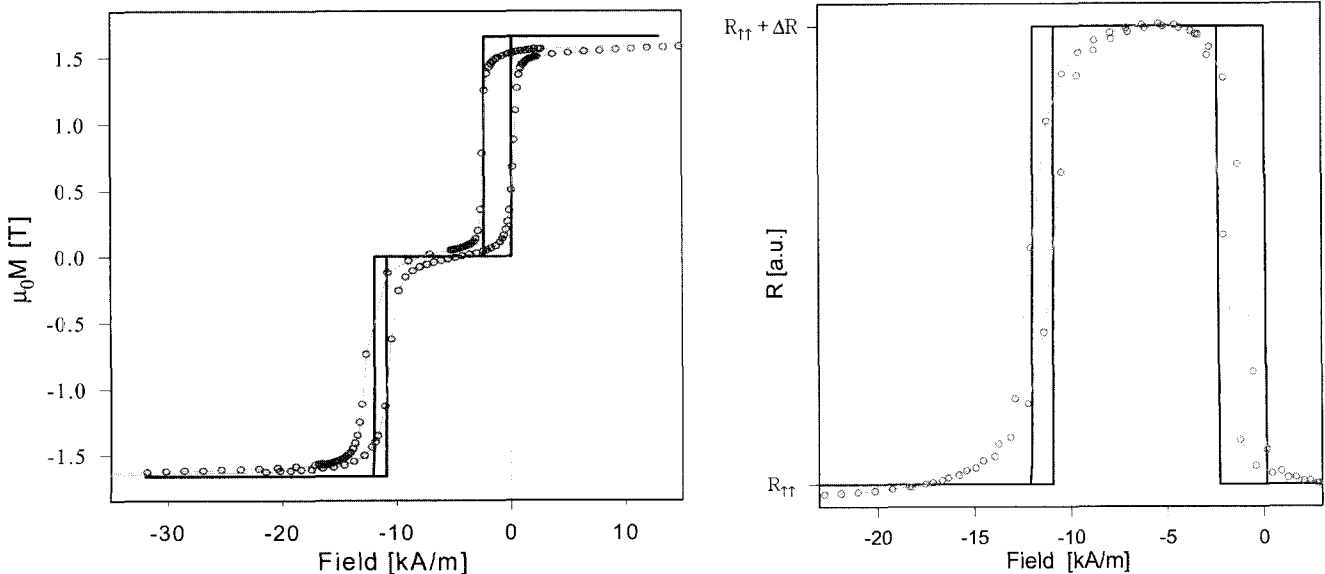

Fig. 2. Spin Valve hysteresis loops: (a) M(H) (b) R(H). Solid line - single domain simulation, circles: experimental data.
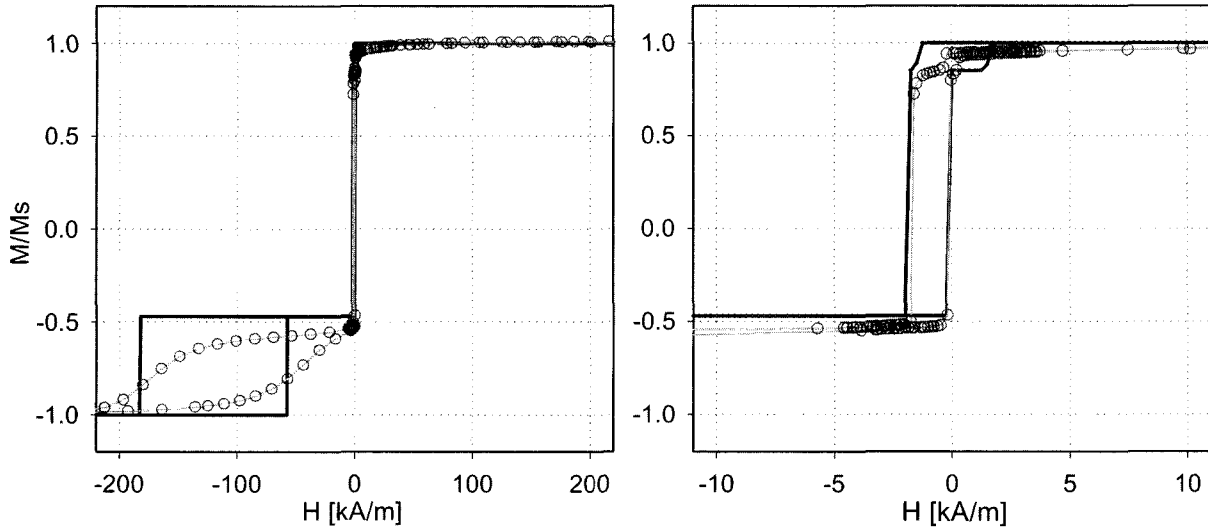
Fig. 3. Annealed MTJ Spin Valve hysteresis loops: (a) major loop, (b) minor loop. Solid line - single domain simulation, circles: experimental data.

by field cooling [4].

Calculations were performed using formula similar to Eq. (1), with additional θ_3 magnetisation angle and additional energy terms for the NiFe buffer with thickness $t_3 = 2$ nm:

$$E(\theta_1, \theta_2, \theta_{AF}) = -J \cos(\theta_2-\theta_1) - J_{EB} \cos(\theta_1-\theta_{AF})$$
$$- t_1\mu_0 M_{S1}(H_X \cos\theta_1 + H_Y \sin\theta_1) - t_2\mu_0 M_{S2}(H_X \cos\theta_2$$
$$+ H_Y\sin\theta_2) - t_3\mu_0 M_{S3}(H_X \cos\theta_3 + H_Y \sin\theta_3) \quad\quad (4)$$
$$- K_1 t_1\cos^2\theta_1 - K_2 t_2\cos^2\theta_2 - K_3 t_3\cos^2\theta_3 - \hat{K}_{AF}\, t_{AF}\cos^2\theta_{AF},$$

This sample exhibits high anisotropy energy $K_{AF} = 360 \times 10^3$ J/m^3. Other parameters are as follows: exchange

constants $J=11 \times 10^{-6}$ J/m^2, $J_{EB}=360 \times 10^{-6}$ J/m^2, uniaxial anisotropy constants $K_1=270$ J/m^3, $K_2=7500$ J/m^3, $K_3=70$ J/m^3. This annealed sample also fulfils condition $K_{AF}\cdot t_{AF} > J_{EB}$ necessary for SV-like characteristics. Comparison of simulated results with experimental magnetic data is shown in Fig. 3a (high field range) and Fig. 3b (low field range).

This sample, before thermal annealing, manifests magnetic behaviour similar to the Pseudo Spin Valve structure (two ferromagnetic layers with different anisotropy). Simulation based on formula (4) gives following results: exchange constants $J=8.5 \times 10^{-6}$ J/m^2, $J_{EB}=320 \times 10^{-6}$ J/m^2, uniaxial anisotropy constants $K_1=280$ J/m^3, $K_2=5200$ J/m^3, $K_3=100$
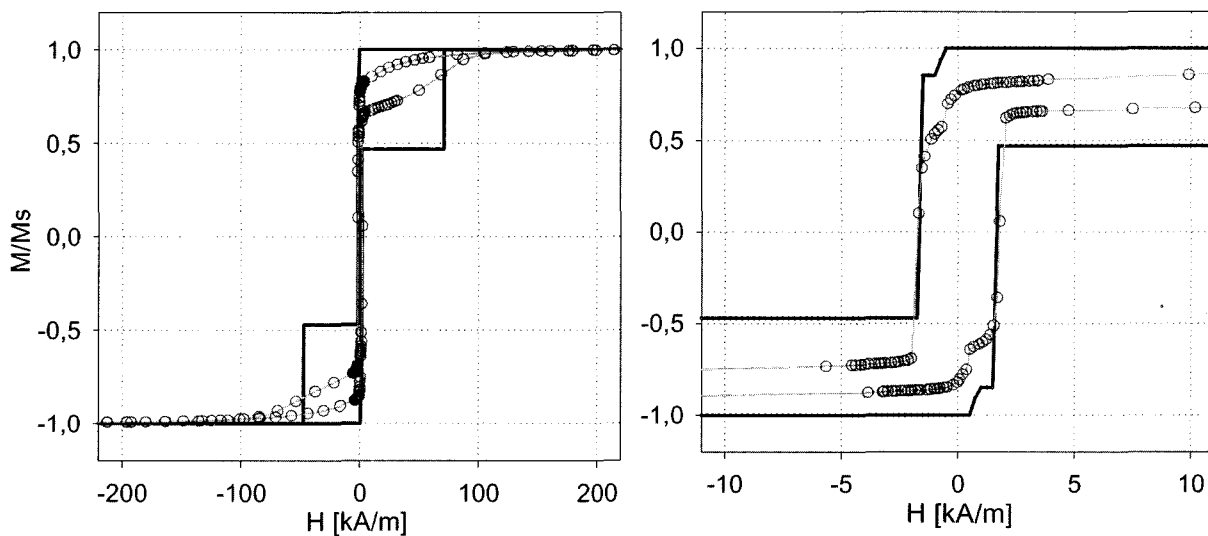

Fig. 4. As-deposited MTJ with Pseudo-Spin Valve hysteresis loops: (a) major loop, (b) minor loop. Solid line - single domain simulation, circles: experimental data.

J/m^3. Fig. 4 shows that measured and simulated magnetisation hysteresis loops are symmetrical due to the low average anisotropy energy $K_{AF}\cdot t_{AF}$ compared to the J_{AF} energy constant.

It can be clearly seen that the single domain model is reproducing simplified shape of hysteresis loop, neglecting the slope originated from multi-domains effects, but providing possibility of quick and easy estimation of basic magnetic parameters.

3. Micromagnetic calculations

The above described single-domain model yields anisotropy constant parameters as effective resultants of crystalline anisotropy, shape anisotropy, magnetostatic anisotropy etc. Neglect of multi-domain structure leads to a rectangular shape of hysteresis loop instead of a smooth one, without effects originated from irregular distribution of local magnetization. More sophisticated studies on the real structures must treat single magnetic layer as a vector field, not as a single magnetic vector. For such vector field we can write the total energy as an integral over entire mesh [5]:

$$E_{tot}(\mathbf{M})$$

$$=\int \left(A(\nabla\mathbf{m})^2-K(\boldsymbol{\alpha}\cdot\mathbf{m})^2-\mu_0\mathbf{M}\cdot\mathbf{H}+\frac{1}{2}(\mu_0\mathbf{M}\cdot\mathbf{H}_d)\right)d\mathbf{v} \quad (5)$$

where A is an exchange energy between neighbouring domains, $\mathbf{m}$ is a unity magnetisation vector $\mathbf{M}/M_S$, $\boldsymbol{\alpha}$ is a unity vector parallel to the easy axis, $\mathbf{H}_d$ is a demagnetising field which should be calculated as an integral of the magnetisation divergence over the whole sample, for each point of the sample. Reconstruction of the hysteresis loop is similar as described for single domain model - for each $\mathbf{H}$ field a local energy minimum should be calculated, which gives an effective field for each point of the sample:

$$\mathbf{H}_{eff}=-\frac{1}{\mu_0}\frac{\delta E_{tot}}{\delta\mathbf{M}} \quad (6)$$

Every magnetic vector will rotate to attain the direction of this effective field, according to the Landau-Lifshitz-Gilbert formula [6]:

$$\frac{\partial\mathbf{M}}{\partial t}=-\gamma(\mathbf{M}\times\mathbf{H}_{eff})-\frac{d\gamma}{M_S}\mathbf{M}\times(\mathbf{M}\times\mathbf{H}_{eff})$$

where γ is a gyromagnetic factor, d is a damping factor of magnetisation precession. If information about dynamic response is not important, damping factor can be set to the high value to speed up calculations. Dynamic cannot
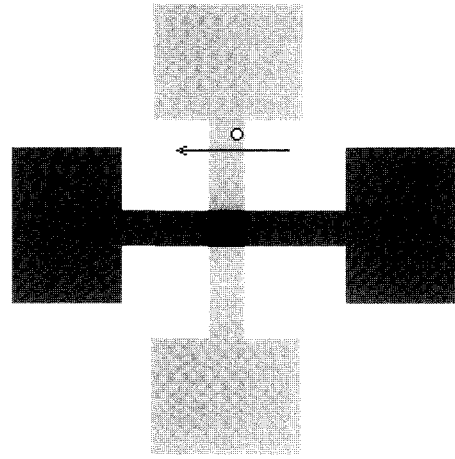

Fig. 5. MTJ MRAM cell arrangement. Magnetic field is in the arrow direction, circle denotes spot of Kerr light.

be completely neglected to avoid large angles between neighbouring magnetisation vectors. Additionally, one can see that discretisation of the sample to the finite elements must be done so as to avoid calculation of artefacts (elements should not be too large), and this implies that the size of simulated sample must have micrometric dimensions. Such calculations require large amount of computer resources. These restrictions can be avoided using boundary conditions, but only for regular sample shapes.

4. Example of the micromagnetic calculations for MTJ electrode

Magnetic Tunnelling Junction described above can be arranged as a basic part of the memory cell in the Magnetic Random Access Memory (Fig. 5). This example of MTJ [7] is formed at the crossing of two electrodes: with pinned layer (bottom) and with free layer (top). Each electrode has large contact for testing of its TMR characteristics. Non-regular shape of these electrodes causes some disturbances of the magnetic reversal process which was studied for the free layer by means of Kerr measurements with 2 μm laser spot diameter [8]. Simulation of the magnetic reversal process of free layer was performed
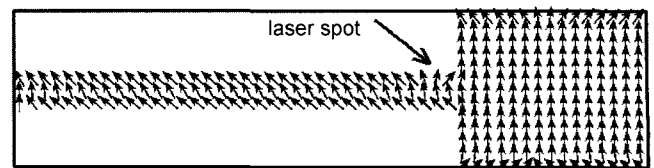

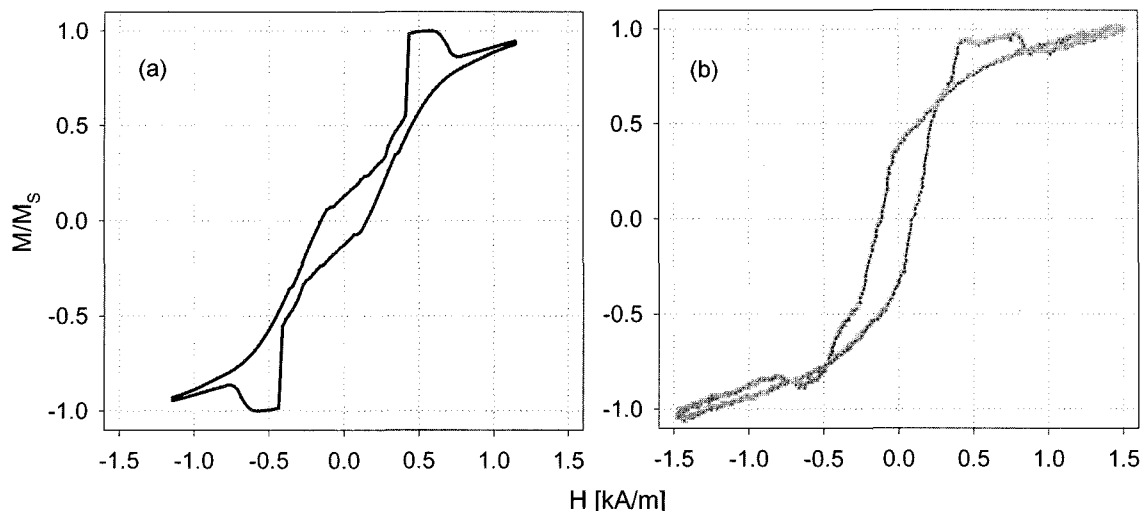**Fig. 6.** Simulation of MTJ electrode - magnetic vector pattern

Fig. 7. Kerr spot measurement of MTJ free layer electrode: (a) simulation, (b) experiment.

by 2D Micromagnetic Interactive Solver tool from the Object Oriented Micromagnetic Framework project [9]. Initial parameters, such as magnetisation saturation and anisotropy constant, were taken from the single domain calculations, described above. Fig. 6 shows an example of the magnetisation vector field for part of the free layer electrode. Such arrays were recorded for each magnetic field step. Simulation of Kerr spot measurement was performed as a calculation of average magnetisation in a given small region of the simulated magnetic vector field. Result of this simulation, compared with the Kerr rotation data, is shown in Fig. 7.

5. Conclusions

One-domain model can be used for fast estimation of basic parameters of the magnetic sample.

Micromagnetic modelling can be used for simulation of several subtle aspects of magnetization process, but due to numerical problems, this method is limited to microscopic scale. These tools can be very useful for predicting behaviour of nanotechnology magnetic elements.

Acknowledgements

This work was supported by Ministry of Scientific Research and Information Technology.

References

[1] B. Dieny, V. S. Speriosu, B. A. Gurney, S. S. P. Parkin, D. R. Wilhoit, K. P. Roche, S. Metin, D. T. Peterson, and S. Nadimi, J. Magn. Magn. Mat. **93**, 101 (1991).

[2] M. Tsunoda and M. Takahashi, J. Appl. Phys. **87**, 4957 (2000).

[3] J. Wrona, M. Czapkiewicz, and T. Stobiecki, J. Magn. Magn. Mater. **196**, 935 (1999).

[4] M. Tsunoda, Y. Tsuchiya, T. Hashimoto, and M. Takahashi, J. Appl. Phys. **87**, 4375 (2000).

[5] W. F. Brown Jr., Micromagnetics, Wiley, New York, 1963.

[6] T. L. Gilbert, Phys Rev. **100**, 1243 (1955).

[7] M. Tsunoda, K. Nishigawa, S. Ogata, and M. Takahashi, Appl. Phys. Lett. **80**, 3135 (2002).

[8] C. G. Kim, V. K. Sankaranarayanan, C. O. Kim, M. Tsunoda, and M. Takahashi, Phys. Stat. Sol. A **201**, 1635 (2004).

[9] M. J. Donahue, and D. G. Porter, OOMMF User's Guide, Interagency Report NISTIR 6376, National Institute of Standards and Technology, Gaithersburg, MD (Sept 1999).